

REVIEW ARTICLE

Observational nuclear astrophysics: Neutron-capture element abundances in old, metal-poor stars

Heather R. Jacobson and Anna Frebel

Kavli Institute for Astrophysics and Space Research and
Department of Physics
Massachusetts Institute of Technology
77 Massachusetts Avenue, Cambridge, MA 02139, USA
E-mail: hrj@mit.edu, afrebel@mit.edu

Abstract. The chemical abundances of metal-poor stars provide a great deal of information regarding the individual nucleosynthetic processes that created the observed elements and the overall process of chemical enrichment of the galaxy since the formation of the first stars. Here we review the abundance patterns of the neutron-capture elements ($Z \geq 38$) in those metal-poor stars and our current understanding of the conditions and sites of their production at early times. We also review the relative contributions of these different processes to the build-up of these elements within the galaxy over time, and outline outstanding questions and uncertainties that complicate the interpretation of the abundance patterns observed in metal-poor stars. It is anticipated that future observations of large samples of metal-poor stars will help discriminate between different proposed neutron-capture element production sites and better trace the chemical evolution of the galaxy.

1. Introduction

1.1. Spectroscopy in Astronomy

The ability to perform spectroscopy on starlight transformed the science of astronomy and the study of cosmic objects. For millennia, astronomers mapped the positions of the stars, traced the orbits of the planets, and recorded the appearance of novae and other phenomena in the sky. But that was as far as they could go: questions such as how far away stars were (parallax being of extremely limited use), and even more fundamentally, what they were made of remained unanswerable until starlight was passed through a telescope and into a spectrograph. It can also be said that spectroscopy first connected astronomy to the sciences of chemistry and physics in profound ways. Whereas Newton united the heavens and Earth with universal laws of motion, studying the spectra of stars helped unravel the secrets of the atom, identified the processes in which elements in the Periodic Table formed, and how the universe became the one we live in now.

Spectroscopy makes this possible by allowing us to see absorption and emission features in starlight as it is spread out by a prism or a grating to form a spectrum. These absorption features are caused by atoms and molecules in the star's

atmosphere absorbing photons coming from the star’s interior at discrete energies (wavelengths/frequencies). As demonstrated by Fraunhofer, Kirchhoff, Bunsen and others in the 19th century, each element or molecule interacts with photons in a unique range of wavelengths, giving each a unique chemical fingerprint. It is therefore possible to identify a species of atom or molecule in a stellar atmosphere based on the presence of its absorption line(s); furthermore, it is possible to infer its abundance (by number) based on the strength of its absorption line(s). Comparing the relative amounts of different chemical species in stars of different ages and locations allows astronomers to trace the history of the production of chemical elements in the universe.

1.2. Chemical Evolution

According to the Big Bang theory, the cosmic fireball that birthed our universe created hydrogen, helium and a fine dusting of lithium. All the other elements in the Periodic Table (typically referred to as “metals” in astronomy) were forged by nuclear reactions within stars, or else in their supernova explosions. Different metals are produced by specific chains of reactions that occur at different ranges of temperatures and densities, and in some cases are controlled by the number of seed nuclei needed for the reactions. Chemical evolution is therefore a product of stellar evolution, as different nucleosynthetic processes turn on and off as stars evolve (see, e.g., the seminal work of Burbidge et al. 1957). Figure 1 shows a simple schematic of this process.

Our Sun, with an age of 4.6 Gyr, reflects the effects of some 8 Gyr of chemical evolution. Many generations of stars enriched the gas from which the Sun and the solar system formed, combining to produce the amount of iron (for example) in our Sun’s atmosphere, in the Earth’s core, and in our blood. Such “layers” of chemical evolution are difficult to disentangle, making it very difficult to directly compare the chemical yields from theoretical supernova models to a star like our Sun. However, as chemical enrichment is a product of successive cycles of star formation and evolution, it is possible to trace the chemical history of our galaxy, and even to study single episodes of chemical enrichment, by studying the oldest stars.

As Figure 1 illustrates, the first stars to form in the universe (so-called Population III stars for historical reasons) formed from pristine clouds of H and He (with maybe tiny amounts of Li), and after their short lifetimes[‡], they polluted interstellar gas with the products of nucleosynthesis in their interiors and in their supernovae. The subsequent generations of stars that formed from this enriched material (correspondingly called Population II) inherited the chemical imprint of the first generation, and then further enriched the interstellar medium with products of their nucleosynthesis in the late stages of their evolution (supernovae, or AGB stars, discussed in more detail later). It is expected that the low-mass stars from this second generation, which were able to form for the first time, still shine in the universe today given their long lifetimes (> 10 Gyr).

1.3. Metal-Poor Stars

It is now worthwhile to more specifically characterize the early, second-generation Population II stars discussed in the previous section. Generically, they are called

[‡] Current theory of star formation in the early universe predicts Population III stars to have been quite massive (10 to 100 M_{\odot}), and therefore all are expected to have exploded as supernovae a few million years after they formed (Bromm & Larson 2004).

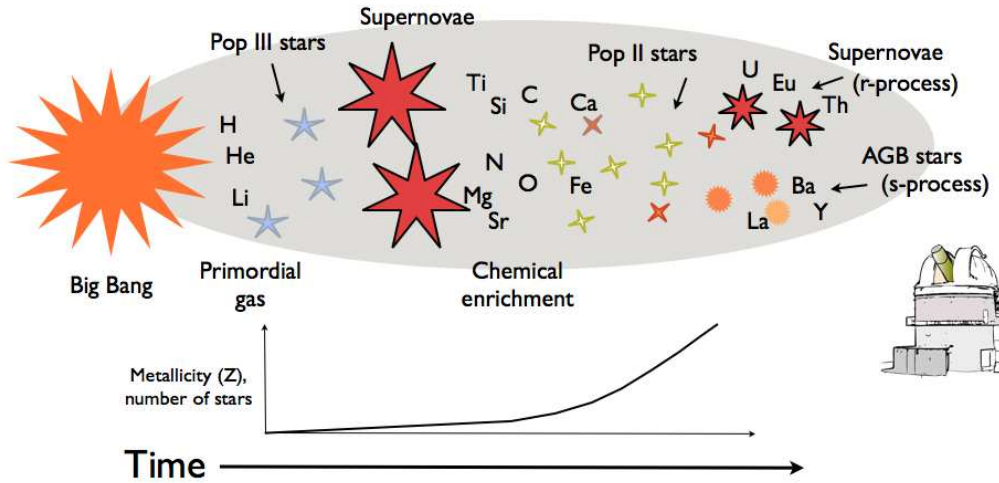


Figure 1. Simple illustration of chemical enrichment of the universe: massive Population III stars form out of primordial gas, explode as supernovae, and enrich the interstellar medium with products of stellar nucleosynthesis. Subsequent cycles of star formation and death (Population II) steadily enrich the universe with metals over time. The first low-mass stars to form in the universe are still observable today. Two main contributors to chemical enrichment after the first stars are 8 – 10 M_{\odot} stars that explode as core-collapse supernovae, and less massive stars that enrich the interstellar medium via strong mass loss and stellar winds (AGB stars). Their nucleosynthetic products, the r-process and s-process elements, are the subject of this review.

“metal-poor” stars, to indicate the relative paucity of the products of stellar nucleosynthesis in their atmospheres, compared to that of the Sun, which almost always serves as the reference. Iron, Fe, is typically used as a proxy for metallicity because the large number of Fe absorption lines present in the optical wavelength regime makes it straightforward to measure. A prefix is often used to illustrate how metal-poor a star is: “extremely metal-poor” ($[\text{Fe}/\text{H}] < -3\%$), “ultra metal-poor” ($[\text{Fe}/\text{H}] < -4$), and “hyper metal-poor” ($[\text{Fe}/\text{H}] < -5$) (Beers & Christlieb 2005). The detailed element abundances of these stars are used to reconstruct the physical and chemical processes of early star and galaxy formation and constrain our understanding of the early universe.

Major topics include:

- The origin and evolution of the chemical elements
- The relevant nucleosynthesis processes and sites of chemical element production
- The nature of the first stars and their initial mass function
- Early star and galaxy formation processes
- Nucleosynthesis and chemical yields of the first/early supernovae
- The chemical and dynamical history of the Milky Way

§ Astronomers employ the $[A/B]$ notation to describe the relative abundances of two elements in a star compared to that in the Sun: $[A/B] = \log_{10}(N_A/N_B) - \log_{10}(N_A/N_B)_{\odot}$. A star with $[\text{Fe}/\text{H}] = -2$, for example, contains a factor 100 fewer Fe atoms by number than the Sun.

- A lower limit to the age of the universe

The sixth item requires large samples of stars covering a wide range of age and metallicity (see Section 5), while the last is made possible by the detection of radioactive elements such as Th and U in selected, individual stars (see Section 4).

As alluded to in the previous section, very different physical conditions are responsible for the production of elements in different regions of the Periodic Table. Studies of metal-poor stars have shown that the production of the light elements (Fe-peak and lighter, atomic number $Z \leq 30$) is decoupled from that of the heavier elements. For example, trends of e.g., [Mg/Fe] versus [Fe/H] for metal-poor stars shows a very small scatter of order 0.1 dex, while the [Ba/Fe] ratios versus [Fe/H] for the same stars have a scatter of >1 dex (Barklem et al. 2005). For the remainder of this review, we focus mainly on what metal-poor stars reveal about the production of the neutron-capture elements ($Z > 38$) and their production sites in the early universe. An extensive earlier review on neutron capture element abundances can also be found in Sneden et al. (2008). For a review of the lighter elements, we refer the reader to Frebel & Norris (2013).

1.4. How Metal-Poor Stars are Found

First though, a brief summary of how metal-poor stars are found and studied is necessary. Metal-poor stars are extremely rare objects which makes finding them a great challenge. Techniques are required to efficiently sift through the large numbers of younger, metal-rich stars to uncover fewer than 0.1% of survivor stars from the early universe. Large-scale systematic searches began with the HK survey by Beers et al. (1985, 1992) which were then superceded by the Hamburg/ESO Survey (Wisotzki et al. 1996; Christlieb et al. 2008). The HES covered ~ 1000 square degrees of the southern sky collecting data of some 4 million point sources.

The low-resolution ($R = \lambda/\Delta\lambda \sim 15 \text{ \AA}$) objective-prism spectra collected in both surveys cover the strong resonance absorption line of calcium, the Fraunhofer “K” line, located at 3933 \AA which can be used as a metallicity indicator. Stars that show a weak CaK line as a function of the surface temperature (temperature affects the line strengths) are selected as candidate metal-poor stars. It is usually assumed that the calcium abundance traces the overall metallicity. To confirm a stars’ low-metallicity nature, additional spectra with higher resolution are required. Those have $R \sim 2000$, are usually obtained with telescopes with 1 to 4 m mirrors, and Figure 2 shows examples. These spectra allow a much more refined measurement of the CaK line strength. Together with the color of the star, they can be turned into a metallicity either via line-strength-color-calibrations (Beers et al. 1999) or through fitting large portions of the spectrum with grids of synthetic spectra of known temperature and metallicity (e.g., Lee et al. 2008).

Once the low-metallicity nature is confirmed from medium-resolution spectra, high-resolution spectra are required for a detailed abundance analysis of many elements, including iron. Spectral lines of Fe and other elements (e.g., Mg, Si, Ti) are very weak and detectable in spectra with $R > 20000$ which are obtained with high-resolution spectrographs on typical ~ 6 to 10 m telescopes.

More recent searches employ slightly modified approaches, such as surveying the sky immediately with medium-resolution spectroscopy using large multi-object spectrographs (the Sloan Digital Sky Survey and its SEGUE follow-up survey, and the LAMOST survey) or selecting metal-poor candidates from photometric survey data.

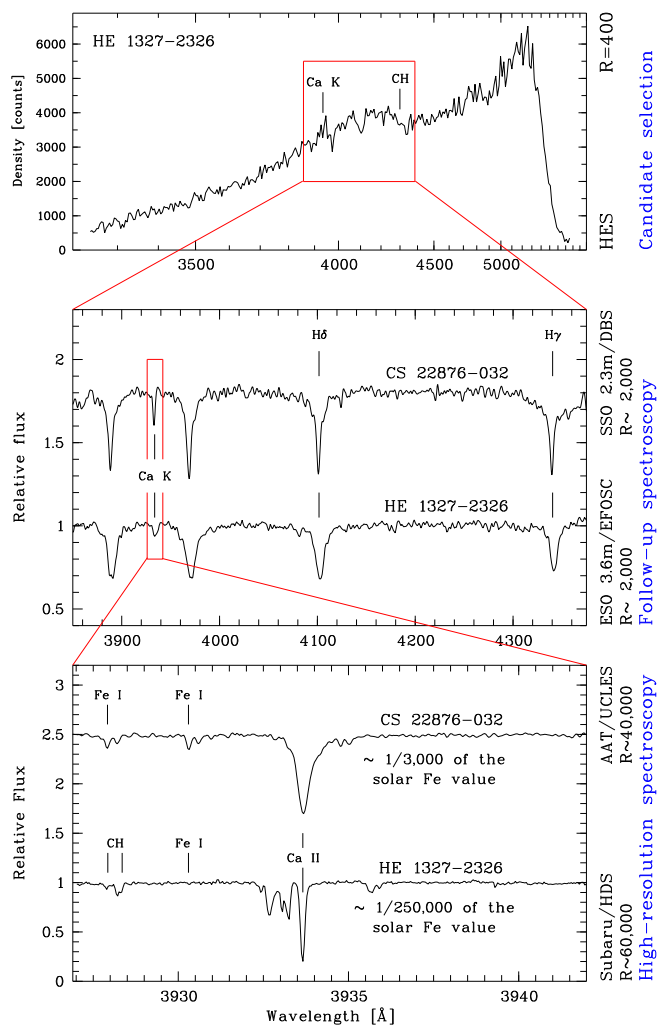


Figure 2. The process of finding a metal-poor star. Stars with weak Ca I K lines are identified in low-resolution spectra (top), and are selected for follow-up with medium-resolution spectroscopy (middle) to get a direct measure of the Ca I K line strength. The most metal-poor stars of this sample are then selected for high resolution followup (bottom), where the abundances of other elements can be determined. Figure taken from Frebel et al. (2005).

The SkyMapper telescope is photometrically surveying the southern sky in specific filter sets (e.g., Bessell et al. 2011) that allow candidate selection in a very efficient way. Follow-up with medium- and high-resolution spectroscopy is still required, though.

2. Neutron-Capture Nucleosynthesis

Elements in the periodic table beyond the iron-peak are primarily formed via the capture of neutrons on to seed nuclei such as iron. This process can occur on two timescales. In the slow neutron-capture process (s-process), the rate of capture of neutrons on to seed nuclei is slow enough to allow the unstable nuclei to β -decay to stable nuclei before subsequent capture. In the rapid neutron-capture process (r-process), the rate of capture is much greater than the rate of β -decay, resulting in the build-up of heavy unstable neutron-rich nuclei that then decay to form heavy, stable nuclei along the “valley of β stability” (Snedden et al. 2008). Each process produced roughly 50% of all the neutron-capture isotopes in the solar system (Arlandini et al. 1999). However, given their different timescales, it is believed that the majority of all elements with $Z \geq 38$ in the early universe (first few stellar generations) were formed via the r-process, with chemical enrichment from low-mass AGB stars coming at later times (e.g., Argast et al. 2000). A significant contribution to the production of elements with $Z \gtrsim 38$ is also predicted to come from massive ($> 8 M_{\odot}$) stars, either by charged particle reactions in core collapse supernovae and/or by the s-process (e.g., Pignatari et al. 2010). In this Section we begin to lay out the nucleosynthesis details of the various neutron-capture processes to then tie them to observations in metal-poor for an understanding of chemical evolution in the next sections.

2.1. The s-Process nucleosynthesis

Detailed reviews of the development of s-process nucleosynthesis theory and observations can be found in, e.g., Busso et al. (1999), Busso et al. (2001), Gallino et al. (1998), and Sneden et al. (2008). Given that much of the s-process evolves along the valley of β stability, most of the neutron capture rates involved can be investigated in the laboratory. As a result, the s-process is qualitatively well-understood and the s-process abundance pattern for the Sun can be well reproduced, especially for $Z > 56$, considering also information from calculations of galactic chemical evolution (e.g., Cameron 1973, Burris et al. 2000, Travaglio et al. 2004). The solar s-process pattern, which serves as the reference to which other stars are compared, shows three distinct peaks in the abundance distribution: the first peak at $Z = 38 - 40$ (Sr, Y, Zr), the second peak at $Z = 56 - 60$ (Ba through Nd), and the third peak at $Z = 82 - 83$, the nuclei at which the s-process ends (Pb, Bi). Elements in each of these peaks are produced by different neutron exposures (Busso et al. 1999; Sneden et al. 2008).

Observations and theory agree that the so-called “main” s-process operates in low- and intermediate mass stars ($\sim 1 - 8 M_{\odot}$; Busso et al. 1999) in the last $\sim 1\%$ of their lifetime as they evolve along the asymptotic giant branch (AGB) in the Hertzsprung-Russell diagram^{||}. During the AGB phase of stellar evolution, a star has an inert carbon oxygen core successively layered with a helium-burning shell, a helium-rich region, a hydrogen-burning shell, and then a convective envelope (see, e.g., Herwig 2005 for a review).

In the classical picture, more than 90% of the neutrons are formed via the $^{13}\text{C}(\alpha, n)^{16}\text{O}$ reaction in between thermal pulses that occur in AGB stars (Straniero et al. 1995). But recent work has indicated that this scenario is likely simplistic and more

^{||} The first sign that neutron capture nucleosynthesis occurs in stars was the detection of the unstable element Tc in an evolved star by Merrill (1952).

neutron-capture regimes may operate, especially at low metallicity (see Lugaro et al. 2012). For this reaction to be activated, a radiative ^{13}C pocket must form after protons from the envelope are mixed down into the intershell layer in order to combine with ^{12}C to form ^{13}C by partial completion of the CN cycle. It is then that the s-process operates. A subsequent convective thermal pulse then mixes the s-process products throughout the He intershell region (e.g., Straniero et al. 1995, Gallino et al. 1998, Herwig 2005). Repeated dredge-up processes finally mix the material from the inner regions of the star to the surface. This sequence of processes happens with each thermal pulse which are on order 10^4 to 10^5 years apart.

Several physical mechanisms have been proposed to explain the formation of the ^{13}C pocket (see Herwig 2005 for a review). Nevertheless, the cause of this mixing remains unclear, and several prescriptions have been developed to simulate the formation of the ^{13}C pocket and the s-process production that occurs in it (e.g., Gallino et al. 1998, Goriely & Mowlavi 2000, Herwig et al. 2003, Bisterzo et al. 2011, Maiorca et al. 2012, Lugaro et al. 2012).

The remaining 10% of neutrons formed in AGB stars are created via the $^{22}\text{Ne}(\alpha, n)^{25}\text{Mg}$ reaction during convective thermal pulses. This reaction results in a higher neutron density compared to that in the ^{13}C pocket ($n_n > 10^{10} \text{ cm}^{-3}$, Herwig 2005 and references therein, Lugaro et al. 2012, Karakas et al. 2012, van Raai et al. 2012). The contribution of this process to the s-process element abundance distribution is smaller than that of the $^{13}\text{C}(\alpha, n)^{16}\text{O}$ reaction. However, the isotopic distribution is greatly affected because of the activation of several branching points along the s-process path. Using the resulting abundance pattern, the conditions in the AGB He intershell can be studied in great detail (e.g., Käppeler et al. 2011).

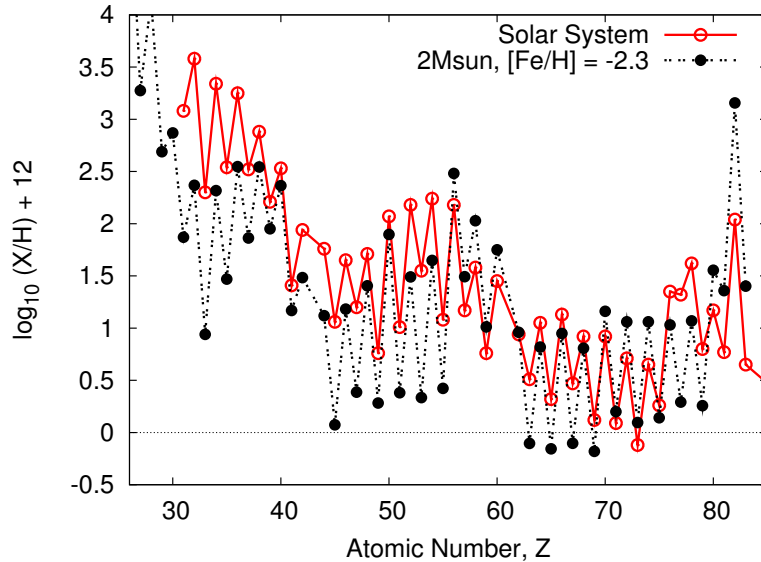


Figure 3. The neutron-capture element abundance pattern of the Sun compared to that of a $2M_{\odot}$ model AGB star with $[\text{Fe}/\text{H}] = -2.3$ (Lugaro et al. 2012). Despite the difference in metallicity, the s-process operates efficiently enough in this metal-poor star to produce s-process abundances equal or greater than the solar system values. Note the enhanced production of lead (Pb, $Z = 82$). Figure from A. Karakas, used with permission.

The s-process efficiency depends on its seed nuclei, therefore the abundance pattern is different in stars of different metallicity (e.g., Gallino et al. 1998, Busso et al. 2001). Figure 3 illustrates this: here, the solar system s-process pattern is compared to that for a model of a low-metallicity AGB star. The low-metallicity AGB star has a larger ratio of neutrons to seed nuclei compared to a solar-metallicity star, and therefore the s-process preferentially produces heavier species. It still results in good agreement between the two patterns for the heavier ($A \gtrsim 170$) species, but larger discrepancies for the lighter species ($90 \leq A \leq 130$) (Karakas 2010; Lugaro et al. 2012). Note also the much larger Pb abundance of the low-metallicity star (see also Section 3.1).

The light s-process elements up to the first peak (which are formed in the “main” s-process in low-mass AGB stars) can also be made by the s-process in intermediate-mass ($>3 M_{\odot}$) AGB stars or in massive ($>8 M_{\odot}$) stars during core He and shell C burning (e.g., Lamb et al. 1977, Busso & Gallino 1985, The et al. 2007, Pignatari et al. 2010). Here, neutrons are created via the $^{22}\text{Ne}(\alpha, n)^{25}\text{Mg}$ reaction. This process generates higher neutron fluxes on shorter timescales than the main s-process described above (e.g., Gallino et al. 1998). Given the shorter lives of massive stars relative to low mass stars, it is possible that massive stars contributed some of the s-process element enrichment in the universe earlier than the main s-process.

Indeed, models of massive, metal-poor and fast-rotating ($\sim 500 - 800 \text{ km s}^{-1}$) stars indicate that rotation-induced mixing within the star leads to production of large amounts of ^{14}N , ^{13}C and ^{22}Ne , the latter of which provides neutrons for the s-process (Pignatari et al. 2008; Frischknecht et al. 2012). Fast rotation can boost s-process element production by orders of magnitude (e.g. for Sr; Chiappini et al. 2011 and references therein). Chemical enrichment from these stars will be discussed further in Section 5.2.

2.2. The r-Process nucleosynthesis

Numerous sites for the r-process have been proposed over the years and generally fall into two broad categories: neutron star - neutron star or neutron star - black hole mergers and supernovae. The merger of compact objects can easily provide the neutron flux needed for rapid neutron-capture to occur (e.g., Lattimer & Schramm 1974, 1976; Freiburghaus et al. 1999; Goriely et al. 2011). However, as pointed out by Argast et al. (2004), the timescales and relative rarity of such events are such that they cannot account for the existence of extremely metal-poor stars exhibiting an r-process signature that presumably formed long before the first neutron-star mergers occurred. Therefore, while they could contribute to some r-process enrichment, neutron star mergers are unlikely to be the main site in the early universe.

Assuming that the r-process takes place during core collapse of massive stars ($8 - 10 M_{\odot}$; e.g., Wanaajo et al. 2003), their explosion mechanisms and properties have also been explored in recent years, but each has its own drawbacks, such as failing to provide sufficient explosion energies, entropies or neutron fluxes to drive the r-process (see, e.g., Cowan & Thielemann 2004; Arnould et al. 2007; Sneden et al. 2008 and references therein). That said, researchers have nonetheless explored the range of possible neutron-capture reactions using the so-called “waiting point method” that is independent of the explosion site. Here, the details of the explosion are not considered, but rather its energy output is used to explore the parameter space of neutron density, electron abundance, neutron flux, and entropy that can produce an abundance pattern

similar to that seen in the Sun as well as metal-poor stars. Some of these models are called the “neutrino wind model” and the “high entropy wind model”, to name two (e.g., Woosley & Hoffman 1992; Wanajo et al. 2001). These studies have found that the neutron densities and entropies required to produce the light neutron-capture species (e.g., Sr, Y, Ba, $Z \approx 38-40$) differ by orders of magnitude from those needed to produce the heavier isotopes (the lanthanides and actinides; Montes et al. 2007; Arcones & Montes 2011; Kratz et al. 2007; Farouqi et al. 2009). While many advances have been made over the last ~ 50 years, the r-process calculations remain a challenging task given the difficulty to obtain experimental data of the most neutron-rich nuclei and the uncertainties relating to the astrophysical site.

3. Neutron-capture element abundances in metal-poor stars

A small subset of metal-poor stars show a strong enhancement of neutron-capture elements compared to iron and lighter elements with $Z \leq 30$. The task at hand then is to identify which nucleosynthesis process was responsible for the creation of these elements that are now observed in those metal-poor stars. The relative enrichment of metal-poor stars by the r- and s-processes compared to Fe can be distinguished by comparing the abundances of elements predominantly produced by either process, or by comparing an element that may be produced by both processes to that produced only in one. For example, lead (Pb) is produced mainly by the s-process, and similarly barium. On the contrary, europium is mainly made by the r-process (e.g., Simmerer et al. 2004). Stars enriched only by the r-process can therefore be identified by their [Pb/Eu] or [Pb/Ba] ratios (e.g., Roederer et al. 2010) or [Ba/Eu] ratios (e.g., Barklem et al. 2005).

3.1. s-Process element abundances

The time-scale over which s-process enrichment occurs after the formation of the first generations of stars is delayed by up to a billion years due to the long main-sequence lifetimes of the first low-mass stars before passing through the AGB phase. 10 – 20% of metal-poor stars in the halo (which can have ages up to 10 – 12 Gyr) display large enhancements of s-process elements (Cohen et al. 2006; Lucatello et al. 2006). The best explanation for the existence of such stars is that their atmospheres were polluted by a slightly more massive binary companion that passed through the AGB phase and transferred s-process material on to them (along with large quantities of carbon, another nucleosynthetic product dredged up to the surface of a star during AGB evolution; Sneden et al. 2008; Lugaro et al. 2012; Placco et al. 2013). Radial velocity studies of such stars indeed show the majority of them to move around a by now unseen companion (Lucatello et al. 2006).

A prominent feature of s-process enriched metal-poor stars is that they show high abundances of the heaviest s-process element, Pb (e.g., Van Eck et al. 2001, Ivans et al. 2005, Cohen et al. 2006, Placco et al. 2013). Lead is the end-product when the s-process is allowed to run to completion. The large Pb abundances of some metal-poor stars are consistent with the theory that Pb is produced in large quantities when the ratio of neutrons to seed nuclei is high (e.g., Gallino et al. 1998), a condition easily met in metal-poor stars (Section 2.1; Figure 3). Aoki et al. (2002) observed s-process element enriched stars that showed a large scatter (>1 dex) in [Pb/Ba] ratios, greater than that predicted by low-metallicity AGB model yields. Such scatter in s-

process element abundances in low-metallicity environments provide useful constraints on AGB stellar evolution models (Herwig 2005; Lugaro et al. 2012). Consequently, the s-process is not a universal process but dependent on the metallicity of the star, and hence, its time of formation in the universe.

For completeness, we note the existence of a small sub-class of metal-poor stars exhibiting neutron-capture elements from both the s- and the r-process. It is further discussed in Sneden et al. (2008).

3.2. *r*-Process element abundances

In contrast to the s-process, the time-scale for neutron-capture and build-up of heavy isotopes via the r-process is of order seconds rather than millennia. The r-process contribution to the neutron-capture isotopes in the solar system is calculated by subtraction of the solar s-process pattern from the total solar system isotopic abundances (as derived from the Sun’s atmosphere and meteorites). The residuals are defined to be “the” r-process (Arlandini et al. 1999; Bisterzo et al. 2011).

A small fraction of stars with $[\text{Fe}/\text{H}] < -2.5$ (e.g., 5% of giant stars; Barklem et al. 2005) show unusually large enhancements in r-process elements ($[\text{r}/\text{Fe}] > 0$). Figure 4 shows the spectra of two stars, one with such large enhancements of neutron-capture element abundances, and another without enhancements. These r-process enriched stars provide important constraints on the site(s) and mechanism(s) of the r-process because they likely formed in the vicinity of a recent supernova event at the earliest times and during which the r-process took place.

Consequently, two general scenarios have been proposed to explain the origin of such large r-process element enhancements in metal-poor stars. The first scenario proposes that they are simply the result of inhomogeneous mixing of r-process material with the ISM, inheriting larger quantities of neutron-capture species compared to others in the same generation (Argast et al. 2000). The second scenario proposes a “local” r-process enrichment due to a close binary companion, (Qian & Wasserburg 2001). Recently, Hansen et al. (2011) presented a test of the second scenario. They carried out a long-term radial velocity study of 17 r-process enhanced giant stars over a 4 year period. Of their sample, 14 had no detectable variation in RV, indicating lack of binarity. Therefore binarity and pollution by a companion are unlikely to explain strong r-process enhancement for the majority of stars. However, the inhomogeneous mixing scenario has its own complications (Section 5.1).

3.2.1. Universal “Main” r-process Stars with unusually strong Eu absorption lines in their spectra are now regularly identified in spectroscopic studies and can be shown to contain large amounts of r-process elements. The first such star to be discovered, CS 22892-052 (Sneden et al. 1996; Sneden et al. 2003), has an element abundance distribution that matches the scaled solar system r-process pattern remarkably well. As the number of r-process enhanced metal-poor stars discovered over the years has grown, many more have been shown to follow the solar system r-process pattern as well (e.g., Sneden et al. 2008). Figure 5 shows examples of this: the abundances of four r-process element enriched stars are shown, along with the solar r-process pattern (solid lines). The agreement is excellent for elements heavier than Ba. This “universality” of the abundance pattern in r-process enriched metal-poor stars and the Sun indicates that the r-process mechanism essentially operates identically wherever and whenever suitable conditions are present. It is present in the very first generations of stars

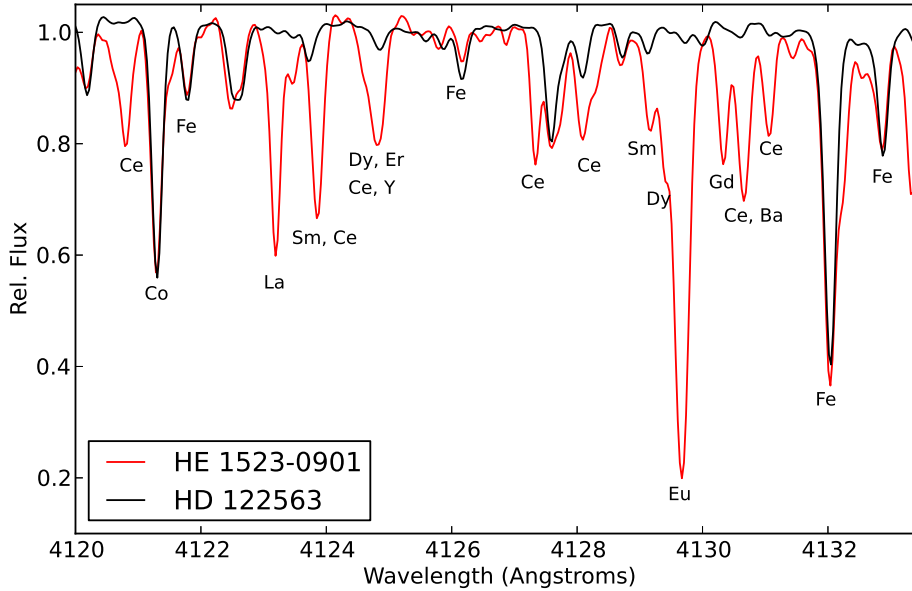


Figure 4. Portions of high resolution ($R = \lambda/\Delta\lambda \approx 30000$) spectra of the r-process element rich star HE 1523–0901 (red) and the r-process element deficient star HD 122563 (black). These two stars have similar $[\text{Fe}/\text{H}]$ values and atmospheric parameters. Various element absorption lines are identified.

and appears unchanged throughout the chemical evolution that culminated in the formation of the Sun.

3.2.2. Deviations from the scaled solar r-process pattern However, not all neutron-capture elements observed in r-process metal-poor stars perfectly follow the scaled solar pattern. The light neutron-capture elements up to barium show deviations in their abundances, as can be seen in Figure 5. These deviations are well documented by now but remain unexplained thus far (e.g., Barklem et al. 2005; Honda et al. 2006, 2007; Roederer et al. 2010; Hansen et al. 2012; Yong et al. 2013). Suggestions include whether these deviations from the scaled solar pattern as well as the scatter found among the known r-process stars reflect observational uncertainties. Many of these elements are difficult to detect in stellar spectra. Also, an additional nucleosynthesis process might be operating in this region producing light neutron-capture elements in addition to the main r-process. This would alter the overall abundance pattern in metal-poor stars compared to that of the sun. Alternatively, there remains the possibility that the production of elements lighter than barium simply is not universally possible.

3.2.3. More deviations: “actinide boost” Another interesting, so far unexplained, phenomenon has appeared among strongly r-process enhanced stars. About a quarter of this group of objects shows thorium abundances that are higher than expected

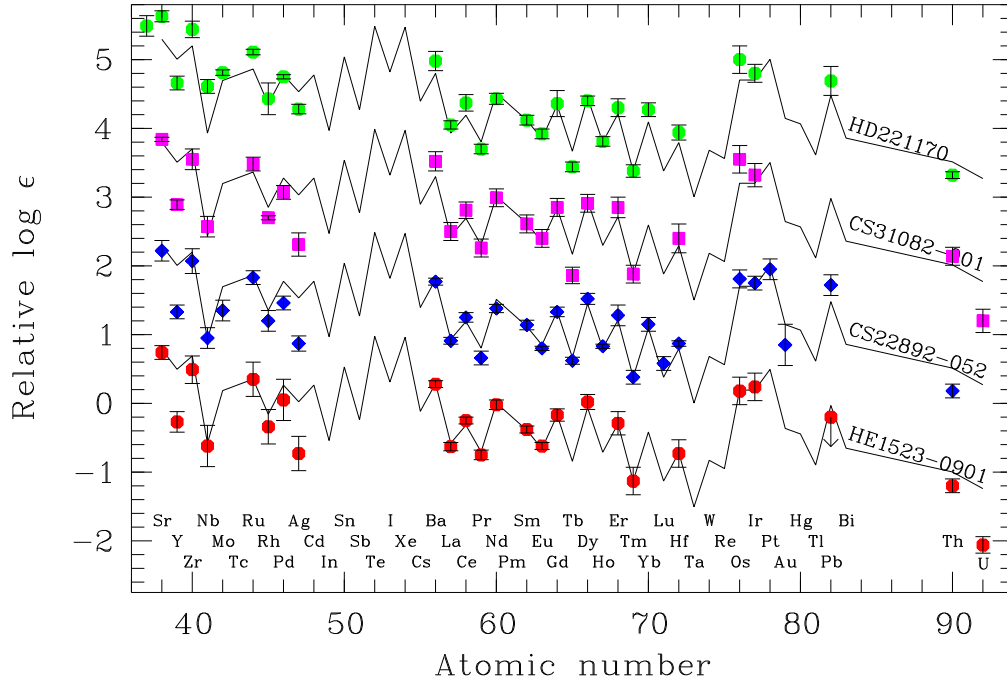


Figure 5. Element abundance patterns of a sample of r-process element enriched stars (points), with the solar r-process pattern scaled to each star’s Eu abundance (solid lines). The agreement between the solar pattern and the stellar abundances is excellent for elements $Z \approx 56 - 72$. However, the agreement with the solar pattern of the lighter elements ($Z \approx 38 - 40$) is not as good. References for the abundances: HD 221170 – Ivans et al. (2006); CS 31082-001 – Hill et al. (2002); CS 22892-052 – Sneden et al. (1996); HE 1523-0901 – Frebel et al. (2007). (Figure adapted from Frebel & Norris 2013.)

compared to other stable r-process elemental abundances and the scaled solar r-process pattern. This behavior has been termed “actinide boost” (Honda et al. 2004; Lai et al. 2007; Hill et al. 2002), and most prominently results in *negative* stellar ages when using the Th/Eu chronometer (see also Section 4) since the decay of thorium has not been lasting since the time of the star’s formation. One explanation may be that these stars show the r-process pattern of two r-process events that occurred at different times – one just prior to the star’s formation and one at a later time in the vicinity of the star. This way, the *pattern* of stable r-process elements would be preserved (albeit not the overall amount), but the radioactive and thus decaying element abundances would be higher than in the case of just the initial r-process abundance level the star was born with. While this explanation is qualitatively straight forward, it remains to be seen how a star could realistically acquire any material from such a hypothesized second r-process event.

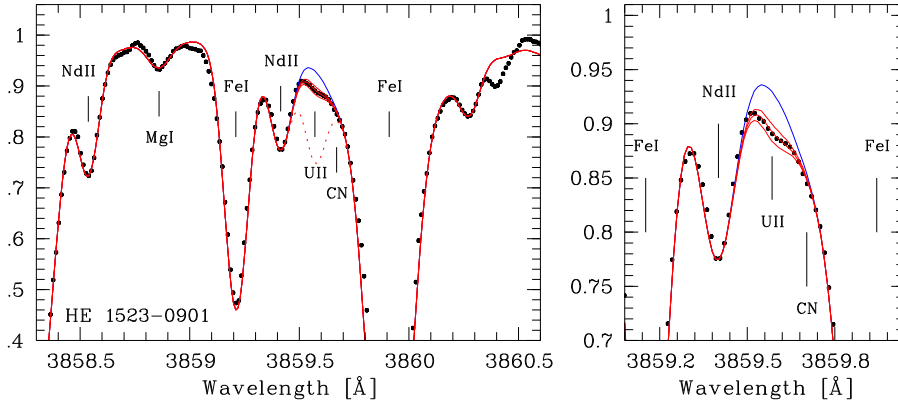


Figure 6. Spectral region around the U II line in HE 1523–0901 (*filled dots*). The right panel is a zoom-in of the region around the U II feature. Overplotted are synthetic spectra with different U abundances. The dotted line in the left panel corresponds to a scaled solar r-process U abundance present in the star if no U were decayed. Figure adapted from Frebel et al. (2007).

4. Cosmo chronometry: age dating the oldest stars

The r-process is responsible for the production of the heaviest elements, including thorium and uranium. These elements are radioactive and have long-lived isotopes, ^{232}Th and ^{238}U , with half-lives of 14 Gyr and 4.5 Gyr, respectively. These half-lives cover cosmic timescales which makes these elements suitable for age measurements, if found in any objects. Indeed, Th and U can be detected in some r-process enhanced metal-poor stars if their level of r-process enhancement is strong enough. Absorption lines of Th are regularly measured but a U detection is very difficult because only one, extremely weak, line is available in the optical spectrum. Figure 6 shows the spectral region around this U line at 3859 Å in the red giant star HE 1523–0901 (Frebel et al. 2007).

Three types of element combinations involving radioactive and naturally occurring stable r-process elements provide chronometers for age measurements in metal-poor stars with r-process enhancement that follow the scaled solar r-process pattern. Examples for stable elements are europium, osmium and iridium. They are abbreviated with “r” in the following equations.

$$\begin{aligned}\Delta t &= 46.7[\log(\text{Th}/r)_{\text{initial}} - \log \epsilon(\text{Th}/r)_{\text{now}}] \\ \Delta t &= 14.8[\log(\text{U}/r)_{\text{initial}} - \log \epsilon(\text{U}/r)_{\text{now}}] \\ \Delta t &= 21.8[\log(\text{U}/\text{Th})_{\text{initial}} - \log \epsilon(\text{U}/\text{Th})_{\text{now}}]\end{aligned}$$

Here, the subscript “initial” refers to the theoretically derived initial production ratio of these elements, while the subscript “now” refers to the observed value of the abundance ratio.

The Th/Eu chronometer can regularly be employed and about a dozen stellar ages of r-process metal-poor stars have been derived this way. The ages range from ~ 11 to 14 billion years which make these stars some of the oldest objects in the universe.

The U/Th chronometer was first measured in CS 31082-001 (Hill et al. 2002) yielding an age of 14 Gyr. However, should be noted, that CS 31082-001 suffers from what has been termed an “actinide boost” (Honda et al. 2004). Compared with the scaled solar r-process it contains too much Th and U. Hence, its Th/Eu ratio yields a negative age. The origin of this issue has yet to be understood. As a result, however, it has become clear that the r-process material in this and other actinide boost stars likely have a different origin than other r-process enhanced metal-poor stars.

Regardless, compared to Th/Eu, the Th/U ratio is more robust to uncertainties in the theoretically derived production ratio due to the similar atomic masses of Th and U (Schatz et al. 2002). Hence, stars displaying Th *and* U are the most valuable old stars. The U measurement in HE 1523–0901 is the currently most reliable one of the only three stars with such detections. The availability of both the Th and U measurements opened up the possibility for the first time to use seven different chronometers, rather than just one (i.e., Th/Eu or U/Th). The averaged stellar age of HE 1523–0901 derived from seven abundance ratios involving combinations of Eu, Os, Ir, Th and U is 13.2 Gyr. Realistic age uncertainties, however, range from ~ 2 to ~ 5 Gyr (Frebel et al. 2007).

Through individual age measurements, r-process objects become vital probes for observational “near-field” cosmology. Importantly, it also confirms that metal-poor stars with similarly low Fe abundances and no excess in neutron-capture elements are similarly old, and that the commonly made assumption about the low mass (0.6 to $0.8 M_{\odot}$) of these survivors is well justified. Finally, these stellar ages provide a lower limit to the age of the galaxy and hence, the universe which is currently assumed to be 13.8 Gyr (Planck Collaboration et al. 2013).

5. Neutron-capture chemical evolution of the galaxy

Up to this point, we have reviewed the neutron-capture abundances of stars showing large enhancements of neutron-capture species that reflect (by now) well-established nucleosynthetic patterns. The vast majority of metal-poor stars in our galaxy do not show such abundance enhancements or clear patterns, but inherited small amounts of neutron-capture material via “standard” chemical evolution (i.e. different processes providing a mix of neutron-capture elements to star forming gas) over subsequent generations of star formation.

Hence, a natural question to ask when considering neutron-capture abundances in metal-poor stars is whether some type of neutron-capture enrichment is seen in all such stars. The answer appears to be yes. Recently, Roederer (2013) carried out a literature survey of some ~ 1400 Milky Way and nearby dwarf galaxy stars, including the most metal-poor (776 stars with $[\text{Fe}/\text{H}] \leq -2.0$) known. Based on a calculation of the detectability of the strongest Sr and Ba lines available in the optical regime, he found that every star studied to date has an abundance measurement or upper limit above the minimum detectable threshold, indicating “that no metal-poor stars have yet been found with sufficiently low limits on $[\text{Sr}/\text{H}]$ or $[\text{Ba}/\text{H}]$ to suggest their birth environment had not been enriched by elements heavier than the iron group. (p. 5)”

In this section, we thus consider the neutron-capture abundance patterns in large samples of metal-poor stars that have arisen as a result of (integrated) galactic chemical evolution and what these global signatures can reveal about the nature of the r-process(es), the s-process, and the competition between r- and s-process element chemical enrichment as a function of time. Figure 7 shows the $[\text{Sr}/\text{Fe}]$ and $[\text{Ba}/\text{Fe}]$

abundance ratios versus $[\text{Fe}/\text{H}]$ for a large sample of metal-poor halo stars. The r-process enhanced stars discussed in Section 3.2 and the s-process enhanced stars discussed in Section 3.1 are indicated by colored symbols; stars that exhibit no

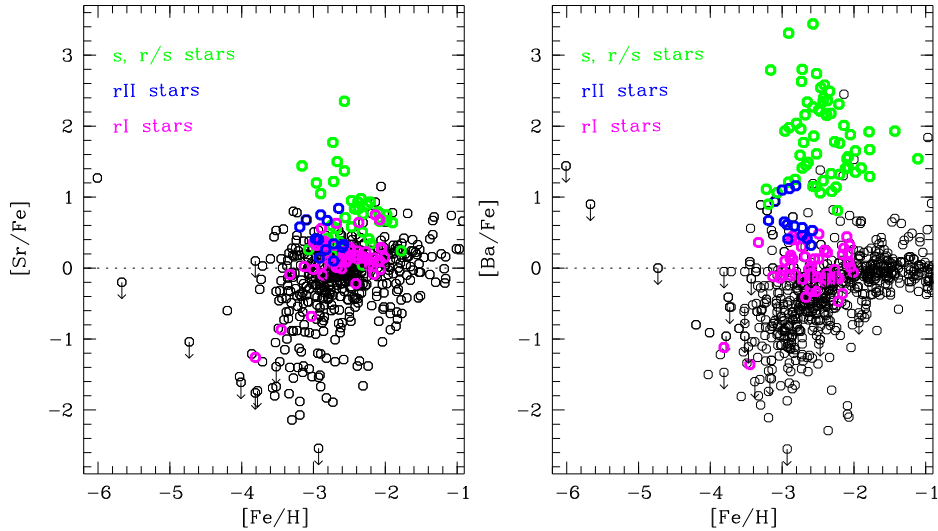


Figure 7. $[\text{Sr}/\text{Fe}]$ and $[\text{Ba}/\text{Fe}]$ versus $[\text{Fe}/\text{H}]$ for metal-poor stars from the catalog of Frebel (2010). R-process enriched stars (where r-I and r-II depict different levels on enhancement), s-process enriched stars, and stars showing both r- and s- enrichment are indicated by colored points. Note the degree of scatter in neutron-capture element abundances even in “normal” metal-poor stars. (Figure adapted from Frebel & Norris 2013.)

5.1. Evolution of r-process enrichment

Since the discovery of metal-poor stars with strong r-process enhancement it has been posited that the r-process must have taken place very early on in the universe. Given that only massive stars contributed to the element production at that time (the low-mass stars had not yet evolved enough to significantly contribute to chemical enrichment) it was proposed that neutrino-driven winds emerging from the proto neutron star during a supernova explosion would be the natural site of the r-process (e.g., Wanajo et al. 2001, 2002). The massive-star-site also explains, at least qualitatively, the existence of neutron-capture material in early gas clouds leading to the formation of metal-poor stars with metallicities of $[\text{Fe}/\text{H}] \lesssim -2.7$. From this metallicity upward, the s-process operating in AGB stars overtakes the global production of neutron-capture elements and subsequent enrichment of the interstellar medium (see Section 5.2 for more details).

Consideration of the r-process as a main source for the early neutron-capture history is also important in the interpretation of the extremely large scatter observed, for example in strontium and barium, as shown in Figure 7. At $[\text{Fe}/\text{H}] \lesssim -3.0$, there are more than three orders of magnitude scatter in the $[\text{Sr}/\text{Fe}]$ and $[\text{Ba}/\text{Fe}]$ abundance ratios, pointing to a large variation in neutron-capture abundances while hardly any variation in iron and presumably other lighter element abundances. The scatter is much beyond any measurement uncertainties which could account for variations on the 0.2 dex level. Moreover, there appears to be a systematic trend of Sr being produced more than Ba, as also apparent from the figure.

Attempts to explain these abundance trends as well as the level of scatter have been numerous, but with few successes. Generally, a consensus is emerging that an additional process or processes may have been at work in the early galaxy, producing preferentially lighter (e.g., Sr) over heavier neutron-capture elements (e.g., Ba). Accordingly, a “lighter element primary process” (LEPP) was proposed (Travaglio et al. 2004) to explain the Sr/Ba ratios observed in metal-poor stars as well as to account for the portion of the solar system abundance pattern between Sr and Ba that is not fully explained by known s-process mechanisms. A contribution by such a process would perhaps also be able to explain, to some extent, the deviations from the scaled solar r-process pattern among light neutron-capture elements in the strongly r-process enhanced metal-poor stars (Section 3.2). Other suggestions include a “weak”, truncated r-process operating in $10 - 20 M_{\odot}$ stars. Here, the entropies and electron fractions reached in the neutrino-driven wind from the proto-neutron star are insufficient to run the r-process to completion, resulting in the preferential build-up for the lighter r-process species (Wanajo & Ishimaru 2005).

An alternative explanation of the overall scatter in neutron-capture element abundances at the lowest metallicities (and hence, earliest times) is that rather than there being multiple formation sites, there is only one site in which the r-process reaches various levels of completion, an extension of the “weak” r-process scenario above. For example, using supernova nucleosynthesis calculations (Woosley et al. 1994), Boyd et al. (2012) modeled a massive ($8 - 40 M_{\odot}$) star undergoing core collapse to a neutron star, with r-process reactions going on in the neutrino driven wind. These reactions may cease abruptly if the neutron star collapses into a black hole, taking some of the r-process element forming regions with it.

The abundance pattern of neutron-capture elements of the metal-poor star HD 122563 (Honda et al. 2006) shows a clear gradient of decreasing abundance with increasing atomic number. This could perhaps be the pattern emerging from this suspected process that produces light neutron-capture elements over heavier ones. Such a truncated r-process indeed provides a reasonable fit to the observed abundances of this heavy neutron-capture element depleted star.

To explain the huge scatter in neutron-capture elements, Aoki et al. (2013) incorporated the truncated r-process scenario of Boyd et al. in the galactic chemical evolution model of Cescutti et al. (2006). They found they were able to reproduce the range of $[\text{Sr}/\text{Ba}]$ ratios found in metal-poor stars. This scenario may also explain the very different levels of scatter of neutron-capture elements compared to α -elements, if the production of α -elements is occurring in layers further out from the proto-neutron star and can therefore more easily escape collapse onto the black hole. Overall, chemical evolution models that incorporate multiple (at least two) r-process sites are better able to reproduce the abundance patterns of metal-poor stars (Qian & Wasserburg 2007). To complicate matters, it is likely that the s-process

operating in fast-rotating massive stars (see Section 5.2) may also contribute to the scatter seen at the lowest metallicities. With more observational data and improved theoretical modeling of the process and sites, the contributions of all these processes can be disentangled.

5.2. Evolution of s-process enrichment

The onset of s-process enrichment in our Galaxy, that is the “time” at which the first intermediate- and low-mass stars had reached the AGB phase and began to pollute their environments with s-process material, has been the subject of careful study. There is some uncertainty in the literature over when this process begins. A study of the relative abundances of Ba and Eu by Burris et al. (2000) showed some indication that s-process enrichment set in by $-2.4 < [\text{Fe}/\text{H}] < -2.1$, but in some stars may appear as early as $[\text{Fe}/\text{H}] \sim -2.75$ ($[\text{Fe}/\text{H}]$ being a “chemical time”.) Simmerer et al. (2004) found signs of its presence at $[\text{Fe}/\text{H}] \sim -2.6$, but remarked on the large spread in s-process element $[\text{X}/\text{Fe}]$ ratios, even at solar $[\text{Fe}/\text{H}]$ in their stellar sample. Similarly, Hansen et al. (2012) found evidence of the s-process at $[\text{Fe}/\text{H}] \sim -2.5$, due to flattening of abundance trends with $[\text{Fe}/\text{H}]$ and general decrease in scatter at that point. However, other studies have found first signs of the s-process enrichment much later, at $[\text{Fe}/\text{H}] \sim -1.5$ (Roederer et al. 2010; Zhang et al. 2010).

The short lifetimes of rapidly-rotating massive metal-poor stars (e.g., Meynet et al. 2006, Hirschi 2007) makes these stars potentially significant contributors to the s-process production in the early universe (recall Section 2.1) before the onset of s-process enrichment through low-mass AGB stars. These spinstar models predict that large amounts of scatter in neutron-capture element-to-iron ratios, as well as in ratios of light (e.g., Sr) to heavy (Ba) element abundances, which is what is seen in metal-poor stars (Figure 7). Chemical evolution models of the galactic halo that include yields of spinstars along with chemical enrichment from $8-10 M_{\odot}$ stars via the main r-process reproduce the scatter in neutron-capture element abundance trends in metal-poor stars very well (Chiappini et al. 2011; Cescutti et al. 2013). Furthermore, Cescutti et al. (2013) posit that the s-process contribution of spinstars in the early universe also provide a natural explanation for why no metal-poor star has yet been observed to lack neutron-capture element abundances (Roederer 2013).

6. Summary and open questions

We have presented an overview of neutron-capture abundance studies of metal-poor stars and how the different groups of stars can help to constrain either individual nucleosynthesis processes such as the r- and the s-process, their sites of operation, and the overall process of chemical evolution that is driven by a variety of sites with time.

The wealth of data on the different neutron-capture processes not only helps to reconstruct the formation and evolution of the heaviest elements, but also opens new questions for which answers have not yet been found. For example, the deviations from the scaled solar r-process pattern remain puzzling both observationally and theoretically. Then, details of the mass transfer events across binary systems and the subsequent dilution processes of s-process material into the atmosphere of the metal-poor stars still observable today are not well understood. However, our interpretations regarding the nature of the s-process at low-metallicity depend in part on knowledge of this process.

Another interesting observational finding is that all the strongly r-process enhanced metal-poor stars found so far exhibit a narrow range in $[\text{Fe}/\text{H}]$ of 0.3–0.4 dex. If the r-process is universal, why do these stars appear at a certain “chemical time”, as put by Hansen et al. (2011)? Some propose this signals the start of a new process at work in the chemical evolution of the universe (e.g., François et al. 2007), or else that these stars only form from a very special type of supernova in which the neutron-capture elements are released via jets, unlike the other elements (Hansen et al. 2011). More generally, no stars with $[\text{Fe}/\text{H}] < -3.5$ have yet been discovered that display any known or characteristic neutron-capture abundance pattern. This raises the question of when exactly the very first neutron-capture events took place in the early universe and whether massive Population III stars produced neutron-capture material, and if so, in what quantities. Finally, abundances of neutron-capture elements with $40 < Z < 56$, i.e. those between the first and second peak, signal that yet other, unidentified neutron-capture processes may have been at work in the early universe. In their analysis of silver and palladium in metal-poor stars, Hansen et al. (2012) found that the abundance ratios of Pd and Ag (e.g., $[\text{Ag}/\text{Fe}]$, $[\text{Ag}/\text{Eu}]$, $[\text{Ag}/\text{Ba}]$) did not match the patterns expected if they were produced by the main r, the weak r, or any s-process channel.

Only with more and better data of existing and to be discovered metal-poor stars will some of these questions be answered. Upcoming telescope projects such as the 25 m Giant Magellan Telescope, when equipped with high-resolution spectrographs, in combination with targets selected from large-scale sky surveys will greatly advance the discovery process of many extremely metal-poor stars to move observational nuclear astrophysics into a new era.

We thank Marco Pignatari for helpful comments and suggestions on parts of the manuscript. Amanda Karakas is also gratefully acknowledged for making Figure 3 for this review, as well as for her comments on the final draft.

References

- Aoki W, Ryan S G, Norris J E, Beers T C, Ando H & Tsangarides S 2002 *ApJ* **580**, 1149–1158.
- Aoki W, Suda T, Boyd R N, Kajino T & Famiano M A 2013 *ApJL* **766**, L13.
- Arcones A and Montes F 2011 *ApJ* **731**, 5.
- Argast D, Samland M, Gerhard O E & Thielemann F K 2000 *A&A* **356**, 873–887.
- Argast D, Samland M, Thielemann F K & Qian Y Z 2004 *A&A* **416**, 997–1011.
- Arlandini C, Käppeler F, Wisshak K, Gallino R, Lugaro M, Busso M & Straniero O 1999 *ApJ* **525**, 886–900.
- Arnould M, Goriely S & Takahashi K 2007 *PhysRep* **450**, 97–213.
- Barklem P S, Christlieb N, Beers T C, Hill V, Bessell M S, Holmberg J, Marsteller B, Rossi S, Zickgraf F J & Reimers D 2005 *A&A* **439**, 129–151.
- Beers T C & Christlieb N 2005 *ARA&A* **43**, 531–580.
- Beers T C, Preston G W & Sackett S A 1985 *AJ* **90**, 2089–2102.
- Beers T C, Preston G W & Sackett S A 1992 *AJ* **103**, 1987–2034.

- Beers T C, Rossi S, Norris J E, Ryan S G & Shefler T 1999 *AJ* **117**, 981–1009.
- Bessell M, Bloxham G, Schmidt B, Keller S, Tisserand P & Francis P 2011 *PASP* **123**, 789–798.
- Bisterzo S, Gallino R, Straniero O, Cristallo S & Käppeler F 2011 *MNRAS* **418**, 284–319.
- Boyd R N, Famiano M A, Meyer B S, Motizuki Y, Kajino T & Roederer I U 2012 *ApJL* **744**, L14.
- Bromm V & Larson R B 2004 *ARA&A* **42**, 79–118.
- Burbidge E M, Burbidge G R, Fowler W A & Hoyle F 1957 *Reviews of Modern Physics* **29**, 547–650.
- Burris D L, Pilachowski C A, Armandroff T E, Sneden C, Cowan J J & Roe H 2000 *ApJ* **544**, 302.
- Busso M & Gallino R 1985 *A&A* **151**, 205–214.
- Busso M, Gallino R, Lambert D L, Travaglio C & Smith V V 2001 *ApJ* **557**, 802–821.
- Busso M, Gallino R & Wasserburg G J 1999 *ARA&A* **37**, 239.
- Cameron A G W 1973 *SSRv* **15**, 121–146.
- Cescutti G, Chiappini C, Hirschi R, Meynet G & Frischknecht U 2013 *A&A* **553**, A51.
- Cescutti G, François P, Matteucci F, Cayrel R & Spite M 2006 *A&A* **448**, 557–569.
- Chiappini C, Frischknecht U, Meynet G, Hirschi R, Barbuy B, Pignatari M, Decressin T & Maeder A 2011 *Nature* **472**, 454–457.
- Christlieb N, Schörck T, Frebel A, Beers T C, Wisotzki L & Reimers D 2008 *A&A* **484**, 721–732.
- Cohen J G, McWilliam A, Shectman S, Thompson I, Christlieb N, Melendez J, Ramirez S, Swennesson A & Zickgraf F J 2006 *AJ* **132**, 137–160.
- Cowan J J & Thielemann F K 2004 *Physics Today* **57**(10), 100000–53.
- Farouqi K, Kratz K L, Mashonkina L I, Pfeiffer B, Cowan J J, Thielemann F K & Truran J W 2009 *ApJL* **694**, L49–L53.
- François P, Depagne E, Hill V, Spite M, Spite F, Plez B, Beers T C, Andersen J, James G, Barbuy B, Cayrel R, Bonifacio P, Molaro P, Nordström B & Primas F 2007 *A&A* **476**, 935–950.
- Frebel A 2010 *Astronomische Nachrichten* **331**, 474.
- Frebel A, Aoki W, Christlieb N, Ando H, Asplund M, Barklem P S, Beers T C, Eriksson K, Fechner C, Fujimoto M Y, Honda S, Kajino T, Minezaki T, Nomoto K, Norris J E, Ryan S G, Takada-Hidai M, Tsangarides S & Yoshii Y 2005 in 'IAU Symposium 228' p. 207.
- Frebel A, Christlieb N, Norris J E, Thom C, Beers T C & Rhee J 2007 *ApJ* **660**, L117–L120.
- Frebel A & Norris J E 2013 in 'Planets, Stars and Stellar Systems Volume 5', Dordrecht: Springer pp. 55–114.
- Freiburghaus C, Rosswog S & Thielemann F K 1999 *ApJL* **525**, L121–L124.
- Frischknecht U, Hirschi R & Thielemann F K 2012 *A&A* **538**, L2.
- Gallino R, Arlandini C, Busso M, Lugaro M, Travaglio C, Straniero O, Chieffi A & Limongi M 1998 *ApJ* **497**, 388.

- Goriely S, Bauswein A & Janka H T 2011 *ApJL* **738**, L32.
- Goriely S & Mowlavi N 2000 *A&A* **362**, 599–614.
- Hansen C J, Primas F, Hartman H, Kratz K L, Wanajo S, Leibundgut B, Farouqi K, Hallmann O, Christlieb N & Nilsson H 2012 *A&A* **545**, A31.
- Hansen T, Andersen J, Nordström B, Buchhave L A & Beers T C 2011 *ApJL* **743**, L1.
- Herwig F 2005 *ARA&A* **43**, 435–479.
- Herwig F, Langer N & Lugaro M 2003 *ApJ* **593**, 1056–1073.
- Hill V, Plez B, Cayrel R, Nordström T B B, Andersen J, Spite M, Spite F, Barbuy B, Bonifacio P, Depagne E, François P & Primas F 2002 *A&A* **387**, 560–579.
- Hirschi R 2007 *A&A* **461**, 571–583.
- Honda S, Aoki W, Ishimaru Y & Wanajo S 2007 *ApJ* **666**, 1189–1197.
- Honda S, Aoki W, Ishimaru Y, Wanajo S & Ryan S G 2006 *ApJ* **643**, 1180–1189.
- Honda S, Aoki W, Kajino T, Ando H, Beers T C, Izumiura H, Sadakane K & Takada-Hidai M 2004 *ApJ* **607**, 474–498.
- Ivans I I, Simmerer J, Sneden C, Lawler J E, Cowan J J, Gallino R & Bisterzo S 2006 *ApJ* **645**, 613–633.
- Ivans I I, Sneden C, Gallino R, Cowan J J & Preston G W 2005 *ApJL* **627**, L145–L148.
- Käppeler F, Gallino R, Bisterzo S & Aoki W 2011 *Reviews of Modern Physics* **83**, 157–194.
- Karakas A I 2010 *MNRAS* **403**, 1413–1425.
- Karakas A I, García-Hernández D A & Lugaro M 2012 *ApJ* **751**, 8.
- Kratz K L, Farouqi K, Pfeiffer B, Truran J W, Sneden C & Cowan J J 2007 *ApJ* **662**, 39–52.
- Lai D K, Johnson J A, Bolte M & Lucatello S 2007 *ApJ* **667**, 1185–1195.
- Lamb S A, Howard W M, Truran J W and Iben, Jr. I 1977 *ApJ* **217**, 213–221.
- Lattimer J M & Schramm D N 1974 *ApJL* **192**, L145–L147.
- Lattimer J M & Schramm D N 1976 *ApJ* **210**, 549–567.
- Lee Y S, Beers T C, Sivarani, T, Allende Prieto, C, Koesterke, L, Wilhelm, R, Re Fiorentin, P, Bailer-Jones, C A L, Norris, J E, Rockosi, C M, Yanny, B, Newberg, H J, Covey, K R, Zhang, H-T & Luo, A-L 2008, *AJ*, **136**, 2022
- Lucatello S, Beers T C, Christlieb N, Barklem P S, Rossi S, Marsteller B, Sivarani T & Lee Y S 2006 *ApJ* **652**, L37–L40.
- Lugaro M, Karakas A I, Stancliffe R J & Rijs C 2012 *ApJ* **747**, 2.
- Maiorca E, Magrini L, Busso M, Randich S, Palmerini S & Trippella O 2012 *ApJ* **747**, 53.
- Merrill P W 1952 *ApJ* **116**, 21.
- Meynet G, Ekström S & Maeder A 2006 *A&A* **447**, 623–639.
- Montes F, Beers T C, Cowan J, Elliot T, Farouqi K, Gallino R, Heil M, Kratz K L, Pfeiffer B, Pignatari M & Schatz H 2007 *ApJ* **671**, 1685–1695.
- Pignatari M, Gallino R, Heil M, Wiescher M, Käppeler F, Herwig F & Bisterzo S 2010 *ApJ* **710**, 1557–1577.

- Pignatari M, Gallino R, Meynet G, Hirschi R, Herwig F & Wiescher M 2008 *ApJL* **687**, L95–L98.
- Placco V M, Frebel A, Beers T C, Karakas A I, Kennedy C R, Rossi S, Christlieb N & Stancliffe R J 2013 *ApJ* **770**, 104.
- Planck Collaboration, Ade P A R, Aghanim N, Armitage-Caplan C, Arnaud M, Ashdown M, Atrio-Barandela F, Aumont J, Baccigalupi C, Banday A J & et al. 2013 *ArXiv e-prints* **1303:5076**.
- Qian Y Z & Wasserburg G J 2001 *ApJL* **552**, L55–L58.
- Qian Y Z & Wasserburg G J 2007 *PhysRep* **442**, 237–268.
- Roederer I U 2013 *AJ* **145**, 26.
- Roederer I U, Cowan J J, Karakas A I, Kratz K L, Lugaro M, Simmerer J, Farouqi K & Sneden C 2010 *ApJ* **724**, 975–993.
- Schatz H, Toenjes R, Pfeiffer B, Beers T C, Cowan J J, Hill V & Kratz K L 2002 *ApJ* **579**, 626–638.
- Simmerer J, Sneden C, Cowan J J, Collier J, Woolf V M & Lawler J E 2004 *ApJ* **617**, 1091–1114.
- Sneden C, Cowan J J & Gallino R 2008 *ARA&A* **46**, 241–288.
- Sneden C, Cowan J J, Lawler J E, Ivans I I, Burles S, Beers T C, Primas F, Hill V, Truran J W, Fuller G M, Pfeiffer B & Kratz K L 2003 *ApJ* **591**, 936–953.
- Sneden C, McWilliam A, Preston G W, Cowan J J, Burris D L & Amorsky B J 1996 *ApJ* **467**, 819–840.
- Straniero O, Gallino R, Busso M, Chiefei A, Raiteri C M, Limongi M & Salaris M 1995 *ApJL* **440**, L85–L87.
- The L S, El Eid M F & Meyer B S 2007 *ApJ* **655**, 1058–1078.
- Travaglio C, Gallino R, Arnone E, Cowan J, Jordan F & Sneden C 2004 *ApJ* **601**, 864–884.
- Van Eck S, Goriely S, Jorissen A & Plez B 2001 *Nature* **412**, 793–795.
- van Raai M A, Lugaro M, Karakas A I, García-Hernández D A & Yong D 2012 *A&A* **540**, A44.
- Wanajo S & Ishimaru Y 2005 *in* V Hill, P François & F Primas, eds, ‘From Lithium to Uranium: Elemental Tracers of Early Cosmic Evolution’ Vol. 228 of *IAU Symposium* p. 435.
- Wanajo S, Itoh N, Ishimaru Y, Nozawa S & Beers T C 2002 *ApJ* **577**, 853–865.
- Wanajo S, Kajino T, Mathews G J & Otsuki K 2001 *ApJ* **554**, 578–586.
- Wanajo S, Tamamura M, Itoh N, Nomoto K, Ishimaru Y, Beers T C & Nozawa S 2003 *ApJ* **593**, 968–979.
- Wisotzki L, Köhler T, Groote D & Reimers D 1996 *A&AS* **115**, 227–233.
- Woolley S E & Hoffman R D 1992 *ApJ* **395**, 202–239.
- Woolley S E, Wilson J R, Mathews G J, Hoffman R D & Meyer B S 1994 *ApJ* **433**, 229–246.
- Yong D, Norris J E, Bessell M S, Christlieb N, Asplund M, Beers T C, Barklem P S, Frebel A & Ryan S G 2013 *ApJ* **762**, 27.
- Zhang J, Cui W & Zhang B 2010 *MNRAS* **409**, 1068–1076.